Mineralogical Magazine, June 1999, Vol. 63(3), pp. 399–411

Ag-Cu exchange equilibria between α-miargyrite, chalcostibite, pyrargyrite, and high-skinnerite: constraints on Ag-Cu mixing in α-miargyrite and chalcostibite

D. E. HARLOV

Projektbereich 4.1, GeoForschungsZentrum, Telegrafenberg, D-14473 Potsdam, Germany

ABSTRACT

Ag-Cu exchange equilibria between α-miargyrite $AgSbS_2$ and pyrargyrite Ag_3SbS_3 and between chalcostibite $CuSbS_2$ and both pyrargyrite and high-skinnerite Cu_3SbS_3 are reported for the temperature range 150–350°C. All of these features are constrained by Ag-Cu exchange experiments (evacuated silica tubes; variable mass ratio) over the temperature range 120–400°C. Chalcostibite is found to take very little Ag into its structure. Utilizing Ag-Cu data from this study as well as the Ag-Cu solution models for pyrargyrite and high-skinnerite, a two-site Ag-Cu non-convergent ordered solution model for α-miargyrite ($W^{A\ Mrg}_{AgCu}$ = 15.0; $W^{B\ Mrg}_{AgCu}$ = 10.0; $\Delta\bar{G}^{*}_{s}$ = 10.0; and $\Delta\bar{G}^{*}_{X_{Cu}s}$ = 14.0 ± 5 kJ/gfw) and a one-site Ag-Cu mixing model for chalcostibite (W^{Chst}_{AgCu} = 25.0 kJ/gfw) are formulated. These results are constrained by a miscibility gap between α-miargyrite and chalcostibite from 225 to 325°C. The mixing model for α-miargyrite is expanded to include As for which α-miargyrite has a limited solubility along the Sb-As join with smithite $AgAsS_2$.

KEYWORDS: Ag-Cu exchange experiments, miargyrite, chalcostibite, pyrargyrite, skinnerite, Ag-Cu solution model, As-Sb solution model.

Introduction

α-MIARGYRITE, $(Ag,Cu)SbS_2$, (monoclinic; space group *C*121; Smith *et al.*, 1997) and pyrargyrite $(Ag,Cu)_3SbS_3$ (rhombohedral; space group *R*3*c*; Harker, 1936; Hocart, 1937) are Ag bearing sulphosalt minerals commonly associated with $(Ag,Cu)_2S$, tetrahedrite-tennantite fahlores $(Cu,Ag)_{10}(Fe,Zn)_2(Sb,As)_4S_{13}$, and polybasite-pearceite $(Ag,Cu)_{16}(Sb,As)_2S_{11}$ all of which are common ores of Ag. At 380°C, α-miargyrite transforms to β-miargyrite (cubic; space group *Fm*3*m*; Keighin and Honea, 1969). α-Miargyrite forms one end of a limited solid solution in As with smithite $AgAsS_2$ along a complex join punctuated by a relatively large miscibility gap between the two phases (Ghosal and Sack, 1995). Smithite is a rare mineral discovered at the Lengenbach quarry in Binnental, Switzerland (Smith and Prior, 1907; Solly, 1905). Pyrargyrite forms one end member of an As-Sb solid solution with proustite $(Ag,Cu)_3AsS_3$. This solid solution is continuous down to at least 90°C (Ghosal and Sack, 1995).

Chalcostibite (orthorhombic; space group $P2_1/n$ $2_1/m$ $2_1/a$; Hofmann, 1935) generally occurs in Cu-Sb rich deposits along with Cu-rich fahlores (Grigas *et al.*, 1976). Skinnerite (Cu_3SbS_3) has been described in only a few localities, principally the Ilimaussaq alkaline intrusion in South Greenland (Karup-Møller, 1974; Karup-Møller and Makovicky, 1974). Here it occurs intergrown with valentinite Sb_2O_3, senarmontite Sb_2O_3, tetrahedrite $(Cu,Ag)_{10}(Fe,Zn)_2Sb_4S_{13}$, chalcostibite, loellingite $FeAs_2$, native antimony, and galena. Structurally, skinnerite possesses a high-to-low reversible phase transition at 122°C which involves doubling the *c*-axis and the appearance of a very slight monoclinic deformation (Makovicky and Skinner, 1972). The synthetic (unquenchable) high-temperature form (>122°C) (high-skinnerite) is orthorhombic, space group *Pnma*, (4 Cu_3SbS_3 formulas per unit cell) whereas the low temperature form is monoclinic, space

group $P2_1/c$ (8 Cu_3SbS_3 formulae per unit cell) (Karup-Møller and Makovicky, 1974). In nature, this phase transformation manifests itself in the form of twinning on (001) which is always present in the low temperature form.

We present results from Ag-Cu exchange experiments between α-miargyrite and pyrargyrite and results from Cu-Ag exchange experiments between chalcostibite and high-skinnerite and between chalcostibite and pyrargyrite. We document unmixing in α-miargyrite, in Ag-Cu exchange with $(Ag_{0.85}Cu_{0.15})_3SbS_3$, into coexisting α-miargyrite and chalcostibite which define the limits of a miscibility gap between α-miargyrite and chalcostibite from 225 to 325°C. Silver-copper solution models for α-miargyrite and chalcostibite are calibrated utilizing previously calibrated Ag-Cu solution models for pyrargyrite and high-skinnerite (Harlov and Sack, 1995*a*).

In essence, this study represents the completion of an experimental and thermodynamic investigation of Ag-Cu and As-Sb mixing properties and stability relations in the Ag-Cu-Sb-As system involving the minerals polybasite-pearcite, pyrargyrite-proustite, skinnerite, chalcostibite, α-miargyrite, smithite, sinnerite ($Cu_6As_4S_9$) and minerals in the Ag_2S-Cu_2S subsystem at 1 bar and temperatures ranging from 75 to 400°C (cf. Harlov and Sack, 1994, 1995*a*, 1995*b*; Harlov, 1995, 1999; and Ghosal and Sack, 1995).

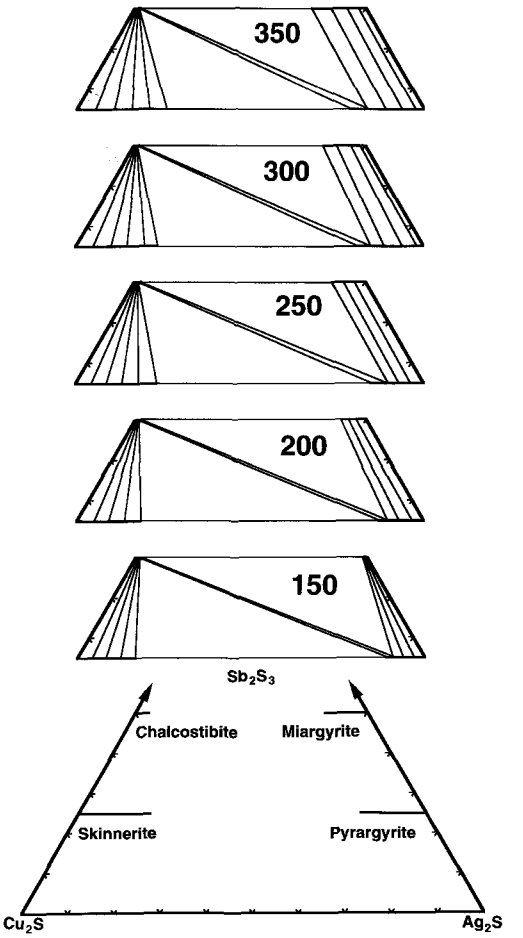

FIG. 1. Phase diagrams for the Ag_3SbS_3-Cu_3SbS_3-$AgSbS_2$-$CuSbS_2$ system at 150, 200, 250, 300 and 350°C. Tie lines (±5%) are inferred from the data presented in Table 1.

Experimental technique

Exchange

The Ag-Cu exchange experiments were performed at 150, 200, 250, 300 and 350°C between α-miargyrite grains and a series of powdered pyrargyrite compositions (X_{Cu} = 0.05–0.15) and between chalcostibite grains and a series of powdered high-skinnerite compositions (X_{Cu} = 0.93, 0.88, 0.85, and 0.80) (Table 1; Figs 1 and 2).

In individual experiments a small grain (500 μm) of end-member α-miargyrite or chalcostibite was immersed in a relatively large amount of the powder and sealed (H_2-O_2 torch) in a 2.0 mm diameter evacuated silica glass tube (oil diffusion pump, $<10^{-4}$ torr). Excess vapour space was minimized with a tightly fitting silica glass rod. In the exchange experiments, due to the fast ion conductor effect of Ag and Cu in sulphides and sulphosalts, the grain totally equilibrated with the powder while the latter, due to its much greater molar amount, (~350 to 1), changed only infinitesimally in composition. This was confirmed by microprobe analysis of the powder after the experiment. The grain composition changed uniformly without any enrichment or depletion of Cu or Ag along the grain rim.

Experimental charges were placed at the exact centre of carefully calibrated 30 or 60 cm horizontal tube furnaces. Abundant glass wool insulation and pumice plugs were used to reduce thermal gradients. During the course of an experiment, temperatures were monitored on a daily basis with a chromal-alumal thermocouple

TABLE 1. Microprobe analyses of α-miargyrite-pyrargyrite, chalcostibite-pyrargyrite, and chalcostibite-skinnerite Ag-Cu exchange experiments from 150–350°C

		Initial molar Cu/(Cu+Ag)		Final $(Ag,Cu)SbS_2$ and $(Cu,Ag)SbS_2$ grain composition and molar Cu/(Cu+Ag) (time, # of analyses, wt.% and standard deviations)											
		Mrg/Chst	Pyr/Skn												
T (C)	Sample	X_{Cu}	X_{Cu}	Hours	# pts	Cu	σ	Ag	σ	Sb	σ	S	σ	Sum	X_{Cu}
150	91-SB-393	0.00	0.05	474	17	0.21	0.03	36.04	0.28	41.54	0.24	22.23	0.11	100.02	0.010
150	91-SB-394	0.00	0.10	474	28	0.26	0.03	36.04	0.22	41.59	0.27	22.16	0.10	100.05	0.012
150	91-SB-395	0.00	0.105	474	40	0.32	0.04	35.98	0.27	41.54	0.23	22.16	0.09	100.00	0.015
150	91-SB-391	1.00	0.93	474	27	25.35	0.21	0.02	0.03	49.09	0.31	25.76	0.08	100.23	0.999
150	91-SB-392	1.00	0.88	474	19	25.25	0.18	0.01	0.01	49.11	0.29	25.90	0.08	100.26	0.999
200	91-SB-382	0.00	0.05	298	9	0.51	0.16	35.61	0.31	41.75	0.42	22.24	0.08	100.11	0.024
200	91-SB-383	0.00	0.10	298	17	0.91	0.70	35.21	1.13	41.59	0.27	22.19	0.11	99.91	0.042
200	91-SB-573	0.00	0.13	1307	17	2.28	0.64	33.59	1.18	41.92	0.26	22.08	0.11	99.86	0.103
200	91-SB-380	1.00	0.93	298	30	25.39	0.18	0.08	0.10	48.88	0.29	25.71	0.13	100.07	0.998
200	91-SB-381	1.00	0.88	298	30	25.32	0.18	0.18	0.13	48.86	0.27	25.72	0.11	100.07	0.996
250	91-SB-473	0.00	0.05	963	17	1.56	0.09	34.44	0.41	41.47	0.37	22.22	0.17	99.68	0.071
250	91-SB-474	0.00	0.10	963	36	3.13	0.20	32.03	0.29	42.18	0.29	22.53	0.11	99.87	0.142
250	91-SB-556*	0.00	0.15	1348	6	3.29	0.06	32.79	0.27	41.25	0.29	21.84	0.06	99.17	0.146
250	91-SB-556*	0.00	0.15	1348	7	25.43	0.30	0.55	0.38	48.06	0.14	25.42	0.11	99.46	0.987
250	91-SB-471	1.00	0.88	963	29	25.29	0.24	0.44	0.12	48.26	0.35	25.65	0.15	99.63	0.990
300	91-SB-371	0.00	0.05	285	19	1.51	0.06	34.48	0.29	41.51	0.25	22.23	0.09	99.72	0.069
300	91-SB-372	0.00	0.10	285	21	2.72	0.40	32.81	0.79	41.80	0.25	22.34	0.10	99.68	0.124
300	91-SB-538*	0.00	0.15	1316	3	4.00	0.07	31.09	0.27	42.43	0.43	22.35	0.08	99.87	0.179
300	91-SB-538*	0.00	0.15	1316	15	25.01	0.28	0.67	0.11	48.71	0.26	25.64	0.16	100.02	0.984
300	91-SB-369	1.00	0.85	285	29	25.39	0.16	0.40	0.12	48.51	0.29	25.50	0.10	99.80	0.991
350	91-SB-359	0.00	0.05	284	13	1.51	0.05	34.33	0.23	41.93	0.31	22.26	0.08	100.03	0.069
350	91-SB-360	0.00	0.10	284	11	3.12	0.03	32.00	0.15	42.40	0.23	22.52	0.08	100.03	0.142
350	91-SB-525	0.00	0.15	1569	4	4.64	0.06	30.40	0.24	42.56	0.26	22.24	0.08	99.84	0.206
350	91-SB-357	1.00	0.80	284	25	25.22	0.22	0.30	0.06	48.92	0.29	25.70	0.12	100.14	0.993

* Grain shows a reaction texture with a chalcostibite rim and remnant miargyrite core

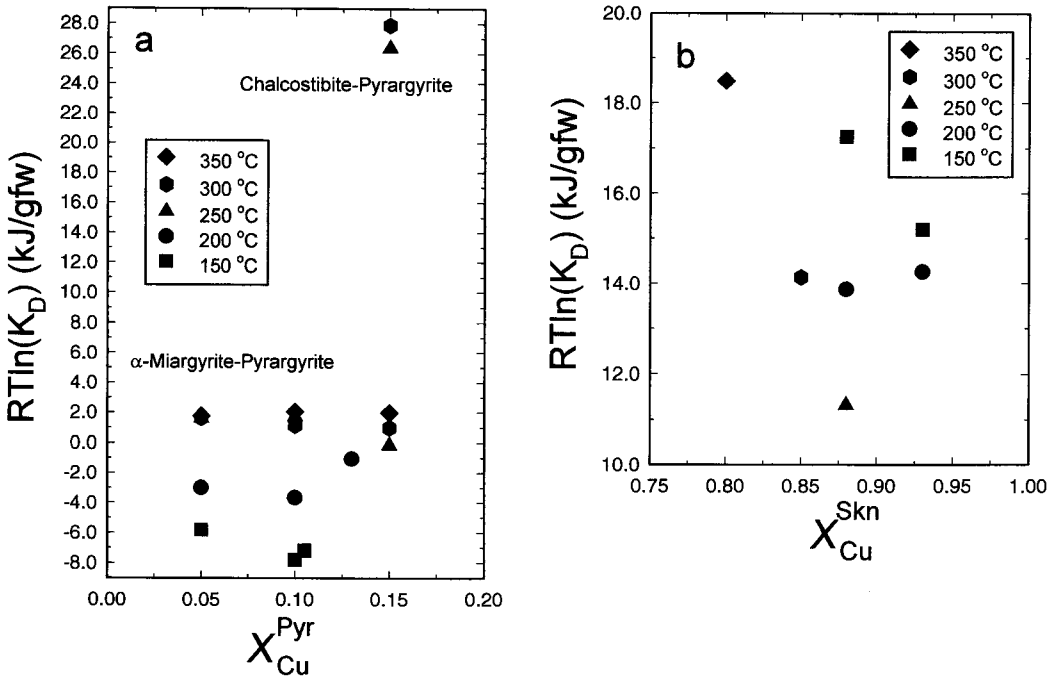

FIG. 2. (*a*) The apparent configurational Gibbs energy of reaction (1), $RT\ln\left[\frac{X^{Mrg}_{Cu}X^{Pyr}_{Ag}}{X^{Mrg}_{Ag}X^{Pyr}_{Cu}}\right]$ expressed as a function of X^{Pyr}_{Cu}, between coexisting α-miargyrite and pyrargyrite, and reaction (2), $RT\ln\left[\frac{X^{Chst}_{Cu}X^{Pyr}_{Ag}}{X^{Chst}_{Ag}X^{Pyr}_{Cu}}\right]$ expressed as a function of X^{Pyr}_{Cu}, between coexisting chalcostibite and pyrargyrite, and (*b*) the apparent configurational Gibbs energy of reaction (3), $RT\ln\left[\frac{X^{Chst}_{Cu}X^{Skn}_{Ag}}{X^{Chst}_{Ag}X^{Skn}_{Cu}}\right]$ expressed as a function of X^{Skn}_{Cu}, between coexisting chalcostibite and high-skinnerite for a series of Ag-Cu exchange experiments at 150, 200, 250, 300 and 350°C (cf. Table 1). These symbols essentially represent either end-member α-miargyrite grains which gained Cu or end-member chalcostibite grains which have gained Ag and thus are half-reversals. Based on previous observations of Ag-Cu exchange equilibria in sulphosalts (cf. Harlov, 1995; Harlov and Sack, 1994; Harlov and Sack, 1995*a,b*) and the Ag-Cu fast ion conductor nature of these sulphosalts, we infer that the Ag-Cu exchange half brackets between α-miargyrite and pyrargyrite; between chalcostibite and high-skinnerite; and between chalcostibite and pyrargyrite, to be relatively close to, if not actually at, the equilibrium points. Error in $RT\ln(K_D)$ for each symbol is ~±0.4 kJ/gfw and reflects a representative uncertainty in X^{Mrg}_{Cu} or X^{Chst}_{Ag} of ±3%.

calibrated to the melting point of sulphur and are accurate to within ±3°C. After quenching in water, the silica glass tube was broken open and the sulphosalt grain was carefully separated out from the powder. The grain was cleaned of clinging powder and mounted in cold setting epoxy. The grain mount was lightly ground down using wetted corundum paper until a suitable cross section of the sulphosalt grain was obtained. Grains were then polished using a 3 and 1 μm diamond paste with an oil lubricant.

Microprobe analysis

All analyses were done on an automated four spectrometer Cameca SX-50 microprobe in the Department of Earth and Atmospheric Sciences at Purdue University using a 10 nA sample current and 20 keV accelerating voltage. Due to the heat sensitive nature of α-miargyrite and chalcostibite, the beam was defocused to a 30 μm diameter. Counting times were limited to 10 s for each element analysis. Synthetic pyrargyrite (Ag_3SbS_3) (Ag) and skinnerite (Cu_3SbS_3) (Cu, Sb, S) were

used as standards for the α-miargyrite and chalcostibite. Three spectrometers (LIF, PET, PET) first counted on Cu (*K*-α), Ag (*L*-α), and S (*K*-α) and then Sb (*L*-α) (PET). Counts were reduced to atom concentrations using a modified ZAF, i.e. 'PAP', correction procedure supplied by Cameca Inc. A sufficient number of analyses (4–40) were taken to evenly cover the surface of each grain. These were averaged to give composite values (Table 1). The analytical precision of the analyses ($\sqrt{N}/N$; N = counts), determined from Poisson statistics of counts on standards, was <1% for Cu, Ag, Sb and S. Based on microprobe analyses of polybasite, pyrargyrite, enargite, and skinnerite internal standards, we believe that analyses of the reacted sulphosalt grains are accurate to within ±3.0% for elements present in concentrations >3 wt.%.

Experimental results

The experimental results provide half brackets for Ag-Cu exchange equilibria between α-miargyrite and pyrargyrite; between chalcostibite and high-skinnerite; and between chalcostibite and pyrargyrite (Table 1; Figs 1 and 2). Due to the limited solid solution composition range in Cu or Ag for these particular sulphosalts, it was only possible to obtain half reversals. However, based on previous observations of Ag-Cu exchange equilibria in sulphosalts (cf. Harlov, 1995; Harlov and Sack, 1994, 1995*a,b*) and the Ag-Cu fast ion conductor nature of these sulphosalts, we infer that the Ag-Cu exchange half brackets between α-miargyrite and pyrargyrite; between chalcostibite and high-skinnerite; and between chalcostibite and pyrargyrite are relatively close to, if not actually at, the actual equilibrium points.

The Ag-Cu exchange equilibria for α-miargyrite-pyrargyrite, $RT\ln\left[\frac{X_{Cu}^{Mrg}X_{Ag}^{Pyr}}{X_{Ag}^{Mrg}X_{Cu}^{Pyr}}\right]$, show a great deal of scatter at low temperatures (150 and 200°C) and relatively little scatter at higher temperatures (250–350°C) (Fig. 2*a*). Reasons for this dichotomy in scatter are most likely due to several factors. Large scatter at low temperatures could be partly due to large relative errors inherent from microprobe analysis of the low Cu concentrations in the α-miargyrite grains (cf. Table 1). A second possible and potentially important factor contributing to this scatter could be a strong temperature dependence on the Ag-Cu ordering between two crystallographically distinct sites in α-miargyrite (cf. Smith *et al.*, 1997: Knowles, 1964) at lower temperatures. At higher temperatures, this ordering is apparently smoothed out with equal abundances of Cu on each site. However, as demonstrated by Sack and Ghiorso (1989) for orthopyroxenes, it is highly unlikely that this scatter could be due to a large value for the standard state entropy for the Ag-Cu exchange reaction between α-miargyrite and pyrargyrite.

The Cu-Ag exchange equilibria between chalcostibite and pyrargyrite:

$$RT\ln\left[\frac{X_{Cu}^{Chst}X_{Ag}^{Pyr}}{X_{Ag}^{Chst}X_{Cu}^{Pyr}}\right], \text{ (Fig. 2}a\text{)},$$

and between chalcostibite and high-skinnerite:

$$RT\ln\left[\frac{X_{Cu}^{Chst}X_{Ag}^{Skn}}{X_{Ag}^{Chst}X_{Cu}^{Skn}}\right], \text{ (Fig. 2}b\text{)}$$

show approximately the same amount of scatter. Based on the crystallographic model of Grigas *et al.* (1976), it is likely that Cu-Ag mixing in chalcostibite occurs on only one site. As a consequence, it is certain that a portion of the scatter in Fig. 2*b* is due almost entirely to the large relative errors inherent from the microprobe analysis of very low Ag concentrations in the chalcostibite grains (cf. Table 1). However, the large scatter in the low temperature experiments (150 and 200°C) could also be partly due to incomplete Ag-Cu equilibration between the chalcostibite grains and the powder, in contrast with the higher temperature experiments, which show a discernible trend.

In two experiments, 91-SB-556 at 250°C and 91-SB-538 at 300°C (Fig. 3), the stable assemblage consists of grains with α-miargyrite cores and thick chalcostibite rims coexisting with pyrargyrite with a Cu content of $X_{Cu} = 0.15$. In these experiments, the original end-member α-miargyrite grain reacted with the Cu-containing pyrargyrite powder such that grains with coexisting Ag-enriched chalcostibite rims and Cu-enriched α-miargyrite cores resulted. Analyses of these cores and rims are given in Table 1. The high temperature (250 and 300°C) and duration of both experiments (over 1300 h) strongly support the idea that these three coexisting phases represent a stable three-phase assemblage between chalcostibite, α-miargyrite and pyrargyrite. As a consequence, this allows for a three-phase region involving α-miargyrite, pyrargyrite and chalcostibite to be located exactly on the Ag_3SbS_3-$AgSbS_2$-$CuSbS_2$ ternary in Fig. 1 at 250 and 300°C as well as to locate the limbs of a miscibility gap between α-miargyrite and chalcostibite at 250 and 300°C in Fig. 4. Three-phase

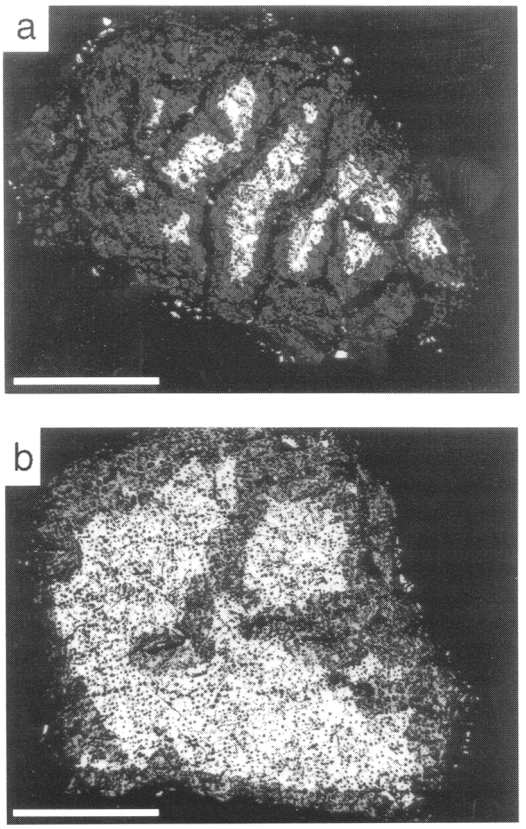

FIG. 3. Back scattered electron images of α-miargyrite grains in equilibrium with powdered pyrargyrite (X_{Cu} = 0.15) from experiments 91-SB-556 at 250°C (*a*) and 91-B-538 at 300°C (*b*). Both experiments show α-miargyrite (white) at the cores of the grains coexisting with extensive chalcostibite rims (light grey). Analyses of coexisting cores and rims are given in Table 1. Scale bar: 500 μm.

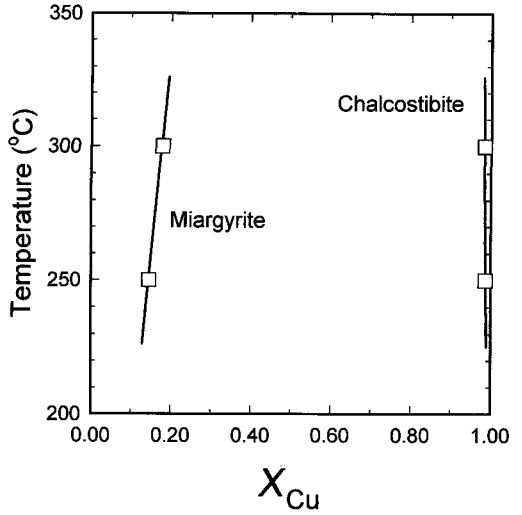

FIG. 4. Measured miscibility gap between α-miargyrite and chalcostibite (white squares) from 225 to 325°C along with the calculated fit (dark line) using the two-site Ag-Cu mixing model for α-miargyrite and a one site Cu-Ag mixing model for chalcostibite at 225, 250, 300 and 325°C. Values for the parameters in these solution models are listed in Table 2.

regions at 150, 200, and 350°C in Fig. 1 were inferred both from Fig. 4 as well as from data in Table 1.

The BSE photographs in Fig. 3 show that the quality of the polish is not very good with extensive plucking of very small grains from the surface of both grains resulting in numerous pores. However it is unlikely that the α-miargyrite or chalcostibite was smeared into the pores of the other mineral during polishing. This was confirmed by taking microprobe analyses of smooth areas between the pores using a 5 μm beam spot with shorter counting times to minimize heat related drift of the Cu and Ag. These analyses gave almost identical Cu and Ag abundances as the 30 μm broad beam analyses for the same region.

Thermodynamic formulation

To evaluate the mixing properties of Ag and Cu in α-miargyrite and chalcostibite, we seek solutions for their energetic properties which simultaneously satisfy the experimental constraint on the partially defined miscibility gap between α-miargyrite and chalcostibite (Fig. 4) and the Ag-Cu exchange reactions between α-miargyrite and pyrargyrite:

$$CuSbS_2 + 1/3Ag_3SbS_3 = AgSbS_2 + 1/3Cu_3SbS_3 \quad (1)$$
α-miargyrite pyrargyrite α-miargyrite pyrargyrite

between chalcostibite and pyrargyrite:

$$CuSbS_2 + 1/3Ag_3SbS_3 = AgSbS_2 + 1/3Cu_3SbS_3 \quad (2)$$
chalcostibite pyrargyrite chalcostibite pyrargyrite

and between chalcostibite and high-skinnerite:

$$CuSbS_2 + 1/3Ag_3SbS_3 = AgSbS_2 + 1/3Cu_3SbS_3 \quad (3)$$
chalcostibite skinnerite chalcostibite skinnerite

(Table 1; Figs. 1,2).

Such solutions are subject to the requirements that differences in the molar Gibbs energies of formation between the end-member Ag and Cu α-miargyrite and chalcostibite:

$$\Delta\bar{G}^{o}_{AgMrg-Chst} = \bar{G}^{o\ Mrg}_{AgSbS_2} - \bar{G}^{o\ Chst}_{AgSbS_2} \quad (4)$$

and

$$\Delta\bar{G}^{o}_{CuChst-Mrg} = \bar{G}^{o\ Chst}_{CuSbS_2} - \bar{G}^{o\ Mrg}_{CuSbS_2} \quad (5)$$

are both negative. That is, since $\bar{G}^{o\ Chst}_{AgSbS_2}$ and $\bar{G}^{o\ Mrg}_{CuSbS_2}$ are both Gibbs free energies of formation for hypothetical end-members which do not actually exist in nature, they would naturally both have much more positive values relative to $\bar{G}^{o\ Mrg}_{AgSbS_2}$ and $\bar{G}^{o\ Chst}_{CuSbS_2}$, respectively, which are Gibbs free energies of formation for end members α-miargyrite and chalcostibite which do exist in nature. These solutions are also subject to the condition that the difference between these quantities is equal to the difference in standard state energies between reactions (1) and (2):

$$\Delta\bar{G}^{o}_{1} - \Delta\bar{G}^{o}_{2} = \Delta\bar{G}^{o}_{AgMrg-Chst} + \Delta\bar{G}^{o}_{CuChst-Mrg} \quad (6)$$

where on a one site basis:

$$\Delta\bar{G}^{o}_{1} = \bar{G}^{o\ Mrg}_{AgSbS_2} + \tfrac{1}{3}\bar{G}^{o\ Pyr}_{Cu_3SbS_3} - (\bar{G}^{o\ Mrg}_{CuSbS_2} + \tfrac{1}{3}\bar{G}^{o\ Pyr}_{Ag_3SbS_3}) \quad (7)$$

and

$$\Delta\bar{G}^{o}_{2} = \bar{G}^{o\ Chst}_{AgSbS_2} + \tfrac{1}{3}\bar{G}^{o\ Pyr}_{Cu_3SbS_3} - (\bar{G}^{o\ Chst}_{CuSbS_2} + \tfrac{1}{3}\bar{G}^{o\ Pyr}_{Ag_3SbS_3}) \quad (8)$$

(cf. Harlov and Sack, 1995*a*; Sack, 1992)

A third difference in the Gibbs free energy between chalcostibite and high-skinnerite on a one site basis may also be written:

$$\Delta\bar{G}^{o}_{3} = \bar{G}^{o\ Chst}_{AgSbS_2} + \tfrac{1}{3}\bar{G}^{o\ Skn}_{Cu_3SbS_3} - (\bar{G}^{o\ Chst}_{CuSbS_2} + \tfrac{1}{3}\bar{G}^{o\ Skn}_{Ag_3SbS_3}) \quad (9)$$

which can directly be related to Reaction (2) and Eqn (8) via the relationship:

$$\Delta\bar{G}^{o}_{3} = \Delta\bar{G}^{o}_{2} + \Delta\bar{G}^{o}_{AgCuPyr-Skn} \quad (10)$$

where:

$$\Delta\bar{G}^{o}_{AgCuPyr-Skn} = \tfrac{1}{3}\bar{G}^{o\ Skn}_{Ag_3SbS_3} - \tfrac{1}{3}\bar{G}^{o\ Skn}_{Ag_3SbS_3} + \tfrac{1}{3}\bar{G}^{o\ Skn}_{Cu_3SbS_3} - \tfrac{1}{3}\bar{G}^{o\ Pyr}_{Cu_3SbS_3} \quad (11)$$

(cf. Harlov and Sack, 1995*a*, their Eqn (5)).

In the ensuing analysis we utilize the solution model for pyrargyrite and high-skinnerite of Harlov and Sack (1995*a*) and the simplifying assumption that the standard state entropies of reactions (1)–(3) are negligible (cf. Sack and Ghiorso, 1989).

α-Miargyrite

In the laboratory and in nature only limited amounts of Cu and As may be substituted into the α-miargyrite structure (Harlov, 1995; Ghosal and Sack, 1995). In the α-miargyrite structure, pyramids consisting of 3 basal sulphurs and an Sb at the apex are bonded together by sharing two sulphur atoms. The coupled pyramids are joined to one another by Ag atoms to form chains running diagonally through the unit cell parallel to the [101] direction. These diagonal chains are connected to each other by a second Ag atom (cf. Smith *et al.*, 1997; Knowles, 1964). Metal cations are equally distributed between two-fold and three-fold co-ordinated sites whereas the semi-metal cations occupy only one type of site (Knowles, 1964). Smith *et al.* (1997) has further refined the three-fold co-ordinated site of Knowles (1964) into two nearly identical three-fold co-ordinated sites which, with respect to our mixing model for miargyrite, we treat as essentially one site.

For an ordered (1:1), two-site α-miargyrite, we assume that the ('vibrational') Gibbs energy, $\bar{G}^{*}$, can be described by a Taylor expansion of second degree in the following composition and ordering variables:

$$X^{Mrg}_{Cu} = \frac{Cu}{Cu + Ag} \quad (12)$$

$$s = X^{A}_{Cu} - X^{B}_{Cu}$$

where X^{Mrg}_{Cu} is the molar ratio and X^{A}_{Cu} and X^{B}_{Cu} are atom fractions of Cu on the 1/2 A and 1/2 B sites in the α-miargyrite formula unit.

Following techniques outlined in Sack (1992), we identify the coefficients of a second degree Taylor expansion:

$$\bar{G}^{*} = g_o + g_{X_{Cu}}X^{Mrg}_{Cu} + g_s s + g_{X_{Cu}X_{Cu}}X^{Mrg^2}_{Cu} + g_{ss}s^2 + g_{X_{Cu}s}X^{Mrg}_{Cu}s \quad (13)$$

with thermodynamic parameters defined in Table 2 and Eqn (13) to obtain the following expression for $\bar{G}^{*}$:

$$\bar{G}^{*} = \bar{G}^{o\ Mrg}_{AgSbS_2}(1 - X^{Mrg}_{Cu}) + \bar{G}^{o\ Mrg}_{CuSbS_2}X^{Mrg}_{Cu} + (\Delta\bar{G}^{*}_{X_{Cu}s} + W^{A\ Mrg}_{AgCu} + W^{B\ Mrg}_{AgCu})X^{Mrg}_{Cu}(1 - X^{Mrg}_{Cu}) + \tfrac{1}{2}(\Delta\bar{G}^{*}_{s} - (W^{B\ Mrg}_{AgCu} - W^{A\ Mrg}_{AgCu}))s + \tfrac{1}{4}(\Delta\bar{G}^{*}_{X_{Cu}s} - (W^{A\ Mrg}_{AgCu} + W^{B\ Mrg}_{AgCu}))s^2 + (W^{B\ Mrg}_{AgCu} - W^{A\ Mrg}_{AgCu})X^{Mrg}_{Cu}s \quad (14)$$

The thermodynamic parameters in Eqn 14 correspond to Gibbs energies of end-member components ($\bar{G}^{o\ Mrg}_{AgSbS_2}$ and $\bar{G}^{o\ Mrg}_{CuSbS_2}$); Gibbs energy of the reciprocal-ordering reaction ($\Delta\bar{G}^{*}_{X_{Cu}s}$) or:

$$AgSbS_2 + CuSbS_2 = Cu^{A}_{0.5}Ag^{B}_{0.5}SbS_2 + Ag^{A}_{0.5}Cu^{B}_{0.5}SbS_2 \quad (15)$$

the Gibbs energy for a Cu-Ag ordering reaction ($\Delta\bar{G}^{*}_{s}$) or:

$$Ag^{A}_{0.5}Cu^{B}_{0.5}SbS_2 = Cu^{A}_{0.5}Ag^{B}_{0.5}SbS_2 \quad (16)$$

and regular solution-type parameters for Cu-Ag ($W^{A\ Mrg}_{AgCu}$ and $W^{B\ Mrg}_{AgCu}$) (Table 2).

Taking into account relations between the atom fractions of Ag and Cu on the A and B sites as well as the composition and ordering variables results in :

$$\begin{aligned} X^{A}_{Cu} &= X^{Mrg}_{Cu} + \tfrac{1}{2}s \\ X^{A}_{Ag} &= 1 - X^{Mrg}_{Cu} - \tfrac{1}{2}s \\ X^{B}_{Cu} &= X^{Mrg}_{Cu} - \tfrac{1}{2}s \\ \text{and} \quad X^{B}_{Ag} &= 1 - X^{Mrg}_{Cu} + \tfrac{1}{2}s \end{aligned} \quad (17)$$

where X^{A}_{Cu} and X^{B}_{Cu} are atom fractions of Cu on the 1/2 A and 1/2 B sites in the α-miargyrite formula unit. We may then write the following expression for the molar configurational entropy, $\bar{S}^{IC}$, for the assumption that Ag and Cu display long range ordering between the A and B sites:

$$\bar{S}^{IC} = -R[\tfrac{1}{2}X^{A}_{Cu}\ln(X^{A}_{Cu}) + \tfrac{1}{2}X^{A}_{Ag}\ln(X^{A}_{Ag}) + \tfrac{1}{2}X^{B}_{Cu}\ln(X^{B}_{Cu}) + \tfrac{1}{2}X^{B}_{Ag}\ln(X^{B}_{Ag})] \quad (18)$$

The molar Gibbs energy, $\bar{G}$, is then defined by the relation:

$$\bar{G} = \bar{G}^{*} - T\bar{S}^{IC} \quad (19)$$

The ordering variable, s, is evaluated by minimizing $\bar{G}$ with respect to s, i.e.

$$\frac{\partial\bar{G}}{\partial s} = \tfrac{1}{2}(\Delta\bar{G}^{*}_{s} - (W^{B\ Mrg}_{AgCu} - W^{A\ Mrg}_{AgCu})) + \tfrac{1}{2}(\Delta\bar{G}^{*}_{X_{Cu}s} - (W^{A\ Mrg}_{AgCu} + W^{B\ Mrg}_{AgCu}))s + (W^{B\ Mrg}_{AgCu} - W^{A\ Mrg}_{AgCu})X^{Mrg}_{Cu} + \tfrac{1}{4}RT[\ln(X^{Mrg}_{Cu} + \tfrac{1}{2}s) - \ln(1 - X^{Mrg}_{Cu} - \tfrac{1}{2}s) - \ln(X^{Mrg}_{Cu} - \tfrac{1}{2}s) + \ln(1 - X^{Mrg}_{Cu} + \tfrac{1}{2}s)] \quad (20)$$

Utilizing the Darken equation (Tangent Intercept Rule) via the following expressions:

$$\mu_{CuSbS_2} = \bar{G} + (1 + X^{Mrg}_{Cu})\left(\frac{\partial\bar{G}}{\partial X^{Mrg}_{Ag}}\right)_{P,T} - s\left(\frac{\partial\bar{G}}{\partial s}\right)$$

and

$$\mu_{AgSbS_2} = \bar{G} - X^{Mrg}_{Cu}\left(\frac{\partial\bar{G}}{\partial X^{Mrg}_{Ag}}\right)_{P,T} - s\left(\frac{\partial\bar{G}}{\partial s}\right) \quad (21)$$

(cf. Sack, 1992; Ghiorso, 1990), we obtain the following expressions for the chemical potentials of α-miargyrite ($AgSbS_2$) and its hypothetical Cu end-member component ($CuSbS_2$):

See below (22)

Finally, a residual plot, whose slope defines the sum $W^{A\ Mrg}_{AgCu} + W^{B\ Mrg}_{AgCu} + \Delta\bar{G}^{*}_{X_{Cu}s}$, can be found by substituting Eqn (22) into the condition of Cu-Ag exchange equilibrium corresponding to reaction (1)

$$\mu^{Mrg}_{CuSbS_2} + \tfrac{1}{3}\mu^{Pyr}_{Ag_3SbS_3} = \mu^{Mrg}_{AgSbS_2} + \tfrac{1}{3}\mu^{Pyr}_{Cu_3SbS_3} \quad (23)$$

and equating $\mu^{Mrg}_{Cu(Ag)_{-1}}$ and $\mu^{Pyr}_{Cu(Ag)_{-1}}$ on a one-site basis or:

$$\bar{Q}^{Mrg-Pyr} = \tfrac{1}{3}RT\ln\left[\frac{a^{Pyr}_{Cu_3SbS_3}}{a^{Pyr}_{Ag_3SbS_3}}\right] + \Delta\bar{G}^{o}_{1} - \tfrac{1}{2}RT\ln\left[\frac{X^{AMgr}_{Cu}X^{BMgr}_{Cu}}{X^{AMgr}_{Ag}X^{BMgr}_{Ag}}\right] - (W^{B\ Mrg}_{AgCu} - W^{A\ Mrg}_{AgCu})s = (\Delta\bar{G}^{*}_{X_{Cu}s} + W^{A\ Mrg}_{AgCu} + W^{B\ Mrg}_{AgCu})(1 - 2X^{Mrg}_{Cu}) \quad (24)$$

where $a^{Pyr}_{Cu_3SbS_3}$ and $a^{Pyr}_{Ag_3SbS_3}$ are activities for pyrargyrite (cf. Harlov and Sack, 1995*a*).

Chalcostibite

The structure of chalcostibite consists of SbS_2 chains running along the *b*-axis which are linked

$$\mu^{Mrg}_{AgSbS_2} = \bar{G}^{o\ Mrg}_{AgSbS_2} + (\Delta\bar{G}^{*}_{X_{Cu}s} + W^{A\ Mrg}_{AgCu} + W^{B\ Mrg}_{AgCu})X^{Mrg2}_{Cu} - \tfrac{1}{4}(\Delta\bar{G}^{*}_{X_{Cu}s} - (W^{A\ Mrg}_{AgCu} + W^{B\ Mrg}_{AgCu}))s^2 - (W^{B\ Mrg}_{AgCu} - W^{A\ Mrg}_{AgCu})X^{Mrg}_{Cu}s + RT[\tfrac{1}{2}\ln(1 - X^{Mrg}_{Cu} + \tfrac{1}{2}s) + \tfrac{1}{2}\ln(1 - X^{Mrg}_{Cu} + \tfrac{1}{2}s)]$$

and

$$\mu^{Mrg}_{CuSbS_2} = \bar{G}^{o\ Mrg}_{CuSbS_2} + (\Delta\bar{G}^{*}_{X_{Cu}s} + W^{A\ Mrg}_{AgCu} + W^{B\ Mrg}_{AgCu})(1 - X^{Mrg}_{Cu})^2 - \tfrac{1}{4}(\Delta\bar{G}^{*}_{X_{Cu}s} - (W^{A\ Mrg}_{AgCu} + W^{B\ Mrg}_{AgCu}))s^2 + (W^{B\ Mrg}_{AgCu} - W^{A\ Mrg}_{AgCu})(1 - X^{Mrg}_{Cu})s + RT[\tfrac{1}{2}\ln(X^{Mrg}_{Cu} + \tfrac{1}{2}s) + \tfrac{1}{2}\ln(X^{Mrg}_{Cu} - \tfrac{1}{2}s)] \quad (22)$$

TABLE 2. Thermodynamic parameters, definitions, and values for miargyrite and chalcostibite

Parameter	Definition	Value (kJ/gfw)
$\Delta\bar{G}^{o}_{1}$	$\bar{G}^{o\ Mrg}_{AgSbS_2} + \frac{1}{3}\bar{G}^{o\ Pyr}_{Cu_3SbS_3} - (\bar{G}^{o\ Mrg}_{CuSbS_2} + \frac{1}{3}\bar{G}^{o\ Pyr}_{Ag_3SbS_3})$	13.5 ± 0.2
$\Delta\bar{G}^{o}_{2}$	$\bar{G}^{o\ Chst}_{AgSbS_2} + \frac{1}{3}\bar{G}^{o\ Pyr}_{Cu_3SbS_3} - (\bar{G}^{o\ Chst}_{CuSbS_2} + \frac{1}{3}\bar{G}^{o\ Pyr}_{Ag_3SbS_3})$	-4.0 ± 0.2
$\Delta\bar{G}^{o}_{3}$	$\bar{G}^{o\ Chst}_{AgSbS_2} + \frac{1}{3}\bar{G}^{o\ Skn}_{Cu_3SbS_3} - (\bar{G}^{o\ Chst}_{CuSbS_2} + \frac{1}{3}\bar{G}^{o\ Skn}_{Ag_3SbS_3})$	-18.2 ± 0.2
$\Delta\bar{G}^{o}_{AgCuPyr-Skn}$	$\frac{1}{3}\bar{G}^{o\ Pyr}_{Ag_3SbS_3} - \frac{1}{3}\bar{G}^{o\ Skn}_{Ag_3SbS_3} + \frac{1}{3}\bar{G}^{o\ Skn}_{Cu_3SbS_3} - \frac{1}{3}\bar{G}^{o\ Pyr}_{Cu_3SbS_3}$*	-14.2 ± 0.2
Regular solution parameters	Relevant joins	
$W^{A\ Mrg}_{AgCu}$	$(Cu)_{0.5}Ag_{0.5}SbS_2$-$CuSbS_2$ $AgSbS_2$-$(Ag)_{0.5}Cu_{0.5}SbS_2$	15.0 ± 0.5
$W^{B\ Mrg}_{AgCu}$	$Ag_{0.5}(Cu)_{0.5}SbS_2$-$CuSbS_2$ $AgSbS_2$-$Cu_{0.5}(Ag)_{0.5}SbS_2$	10.0 ± 0.5
W^{Chst}_{CuAg}	$CuSbS_2$-$AgSbS_2$	25.0 ± 0.5
Reciprocal and reciprocal-ordering parameters	Relevant equilibria	
$\Delta\bar{G}^{*}_{s}$	$Ag^{A}_{0.5}Cu^{B}_{0.5}SbS_2 = Cu^{A}_{0.5}Ag^{B}_{0.5}SbS_2$	10.0 ± 0.5
$\Delta\bar{G}^{*}_{X_{Cu}s}$	$AgSbS_2 + CuSbS_2 = Cu^{A}_{0.5}Ag^{B}_{0.5}SbS_2 + Ag^{A}_{0.5}Cu^{B}_{0.5}SbS_2$	14.0 ± 0.5

* (cf. Harlov and Sack, 1995*a*)

together by Cu atoms into double planar layers. The Sb atoms have three nearest S neighbours and form a trigonal co-ordinated pyramid with the Sb atom at the apex (Hofmann, 1935). According to Grigas *et al.* (1976) and Hoffman (1935), Cu and Ag mix on only one site in the chalcostibite crystallographic structure. As a consequence, Cu-Ag mixing in chalcostibite may be approximated by a simple one-site Cu-Ag solution model:

$$\bar{G} = \bar{G}^{o\ Chst}_{AgSbS_2}(1 - X^{Chst}_{Cu}) + \bar{G}^{o\ Chst}_{CuSbS_2}X^{Chst}_{Cu} + W^{Chst}_{CuAg}X^{Chst}_{Cu}(1 - X^{Chst}_{Cu}) + RT[X^{Chst}_{Cu}\ln(X^{Chst}_{Cu}) + (1 - X^{Chst}_{Cu})\ln(1 - X^{Chst}_{Cu})] \quad (25)$$

or

$$\mu^{Chst}_{CuSbS_2} = \mu^{o\ Chst}_{CuSbS_2} + W^{Chst}_{CuAg}(1 - X^{Chst}_{Cu})^2 + RT\ln(X^{Chst}_{Cu})$$

and

$$\mu^{Chst}_{AgSbS_2} = \mu^{o\ Chst}_{AgSbS_2} + W^{Chst}_{CuAg}X^{Chst^2}_{Cu} + RT\ln(1 - X^{Chst}_{Cu}) \quad (26)$$

Substituting these chemical potential equations for the chalcostibite Cu and Ag end-member components into the statement of the condition of Ag-Cu exchange equilibrium for chalcostibite and pyrargyrite (Reaction 2):

$$\mu^{Chst}_{CuSbS_2} + \tfrac{1}{3}\mu^{Pyr}_{Ag_3SbS_3} = \mu^{Chst}_{AgSbS_2} + \tfrac{1}{3}\mu^{Pyr}_{Cu_3SbS_3} \quad (27)$$

we obtain an expression (after equating $\mu^{Chst}_{Ag(Cu)_{-1}}$ and $\mu^{Pyr}_{Ag(Cu)_{-1}}$ on a one-site basis) for a residual function, $\bar{Q}^{Chst-Pyr}$, whose slope corresponds to the regular-solution parameter W^{Chst}_{CuAg}:

$$\bar{Q}^{Chst-Pyr} = \tfrac{1}{3}RT\ln\left[\frac{a^{Pyr}_{Ag_3SbS_3}}{a^{Pyr}_{Cu_3SbS_3}}\right] - \Delta\bar{G}^{o}_{2} - RT\ln\left[\frac{1-X^{Chst}_{Cu}}{X^{Chst}_{Cu}}\right] = -W^{Chst}_{CuAg}(1 - 2X^{Chst}_{Cu}) \quad (28)$$

Similarly, for Cu-Ag exchange between chalcostibite and high-skinnerite (Reaction 3), substituting in the chemical potentials for chalcostibite and skinnerite results in:

$$\mu^{Chst}_{CuSbS_2} + \tfrac{1}{3}\mu^{Skn}_{Ag_3SbS_3} = \mu^{Chst}_{AgSbS_2} + \tfrac{1}{3}\mu^{Skn}_{Cu_3SbS_3} \quad (29)$$

we obtain a similar expression (after equating $\mu^{Chst}_{Ag(Cu)_1}$ and $\mu^{Skn}_{Ag(Cu)_1}$ on a one-site basis) for a residual function, $\bar{Q}^{Chst-Skn}$, whose slope also corresponds to the regular-solution parameter W^{Chst}_{CuAg}:

$$\bar{Q}^{Chst-Skn} = \tfrac{1}{3}RTln\left[\frac{a^{Skn}_{Ag_3SbS_3}}{a^{Skn}_{Cu_3SbS_3}}\right] - \Delta\bar{G}^{o}_{3} - RTln\left[\frac{1-X^{Chst}_{Cu}}{X^{Chst}_{Cu}}\right]$$
$$= - W^{Chst}_{CuAg}(1 - 2X^{Chst}_{Cu}) \quad (30)$$

where $a^{Skn}_{Ag_3SbS_3}$ and $a^{Skn}_{Cu_3SbS_3}$ are taken from Harlov and Sack (1995*a*). The y-intercept for this slope, $\Delta\bar{G}^{o}_{3}$, is related to $\Delta\bar{G}^{o}_{2}$ via Eqn. (10).

Results and discussion

To obtain feasible solutions for the α-miargyrite and chalcostibite mixing parameters, it is necessary to simultaneously satisfy the constraints on all Ag-Cu exchange data (Eqns 23, 27 and 29; Table 1). In addition, it is necessary to reproduce the α-miargyrite-chalcostibite miscibility gap in Fig. 4 by evaluating the slope of a line drawn tangentially to the $\bar{G}$ energy surfaces for α-miargyrite and chalcostibite plotted as a function of X_{Cu} and temperature. Although there are numerous possible combinations of energetic parameter values which are consistent with the miscibility gap constraints in Fig. 4, only one of these combinations will also satisfy the residual slope for the Ag-Cu α-miargyrite-pyrargyrite, chalcostibite-pyrargyrite, and chalcostibite-high-skinnerite exchange data presented in Fig. 5. In Fig. 5 and Table 2 we present the parameter values for this solution. Maximal errors for the parameter values associated with this solution have been estimated by examining tolerances of fits to the α-miargyrite-chalcostibite miscibility gap (Fig. 4) and Ag-Cu exchange data (Fig. 5) with variations in individual parameter values. Calculation of residual slopes from Ag-Cu exchange data for miargyrite-pyrargyrite, chalcostibite-pyrargyrite, and chalcostibite-skinnerite (cf. Eqns 24, 28 and 30) is done such that the residual plots for miargyrite-pyrargyrite and chalcostibite-pyrargyrite are internally consistent with a y-intercept of 0. The intercept for the chalcostibite-skinnerite residual plot is separated from that of chalcostibite-pyrargyrite by a difference equal to $\Delta\bar{G}^{o}_{AgCuPyr-Skn}$ in Eqn 11. It is obvious from Fig. 5 that a linear fit to the α-miargyrite data is at best a first approximation. The low temperature points at high $(1 - 2X_{Cu})$ have a steeper slope than the higher temperature points at lower values of $(1 - 2X_{Cu})$. The main contribution to this difference in slope is most likely from a strong temperature dependence for Cu-Ag ordering in α-miargyrite at low temperatures as opposed to higher temperatures where ordering between Cu and Ag is apparently less pronounced. However it is beyond the scope of this study to attempt some sort of polynomial fit to the Ag-Cu exchange data for miargyrite-pyrargyrite in Fig. 5. Such a fit would result in additional complexities in an already complex solution model for α-miargyrite, well beyond the scope of the data presented in this paper.

We have inferred that α-miargyrite displays an ordered distribution of Cu and Ag between two crystallographically distinct, equally populated sites designated A and B. The suggestion that α-miargyrite displays a disordered Cu-Ag distribution is not viable because it is impossible to satisfy the miscibility gap constraints without inducing a strong temperature dependent scatter to the residual function, $\bar{Q}$, describing Cu-Ag partitioning between α-miargyrite and pyrargyrite (Fig. 5). This scatter is eliminated with the assumption that Cu is preferentially concentrated on the B site ($\Delta\bar{G}^{*}_{s}$ = 10 kJ/gfw; Eqn 16). This observation is also consistent with the fact that $W^{A\ Mrg}_{AgCu}$ has a larger value than $W^{B\ Mrg}_{AgCu}$ (Table 2). A positive value of 14.0 kJ/gfw for $\Delta\bar{G}^{*}_{X_{Cu}s}$ (Eqn 15) is indicative that miargyrite is willing to take in only very limited amounts of Cu on either the A or B site which is also consistent with the relatively large values of both $W^{A\ Mrg}_{AgCu}$ and $W^{B\ Mrg}_{AgCu}$ and with the observation that in nature, Cu substitution for Ag in miargyrite is very low, generally <1% (cf. Birch, 1981, 1992; Sugaki *et al.*, 1982, 1984, 1986; Kaspar *et al.*, 1983, 1985; Nakayama, 1986; Kaspar *et al.*, 1991).

Similarly, chalcostibite takes in very limited amounts of Ag, as measured by the relatively large value for W^{Chst}_{CuAg} which is of magnitude similar to the regular solution parameters, $W^{A\ Mrg}_{AgCu}$ and $W^{B\ Mrg}_{AgCu}$, in miargyrite (Table 2). This observation is reflected in the steepness of the chalcostibite miscibility gap limb as well as in the small compositional range in Ag for $(Cu,Ag)SbS_2$.

α-Miargyrite presents a relatively complicated phase diagram with smithite along the Sb-As join characterized by a moderately broad miscibility gap between the two phases (cf. Ghosal and Sack,

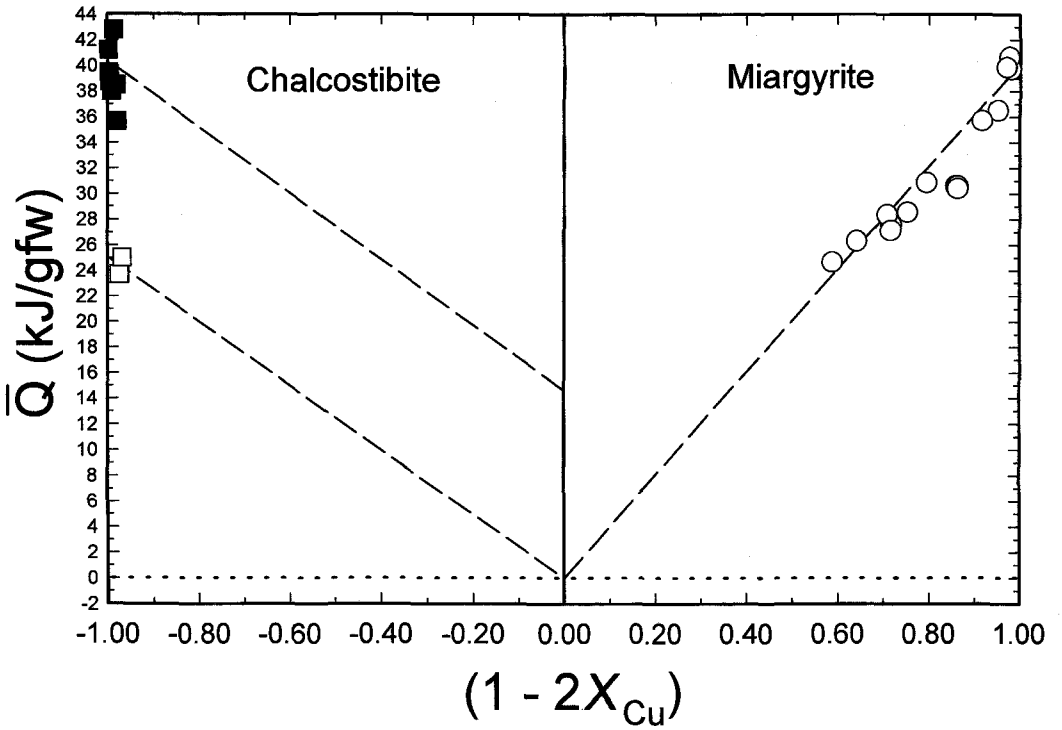

FIG. 5. Residual $\bar{Q}$ plots of Ag-Cu exchange data between α-miargyrite and pyrargyrite (open circles) (Eqn 24) plotted as a function of $(1 \quad 2X_{Cu}^{Mrg})$; and between chalcostibite and pyrargyrite (open squares) (Eqn 28); and between chalcostibite and high-skinnerite (closed squares) (Eqn. 30), both as a function of $(1 \cdot 2X_{Cu}^{Chst})$. Slopes of calculated lines correspond to $W_{AgCu}^{A\ Mrg} + W_{AgCu}^{B\ Mrg} \quad \Delta\bar{G}^{*}_{X_{Cu}s}$ for α-miargyrite and W_{CuAg}^{Chst} for chalcostibite on a one-site basis. Calculation of residual slopes from Ag-Cu exchange data for α-miargyrite-pyrargyrite, chalcostibite-pyrargyrite, and chalcostibite-high-skinnerite (cf. Eqns 24, 28 and 30) is done such that the residual plots for α-miargyrite-pyrargyrite and chalcostibite-pyrargyrite are internally consistent with a y-intercept of 0. The intercept for the chalcostibite-high-skinnerite residual plot is separated from that of chalcostibite-pyrargyrite by a difference equal to $\Delta\bar{G}^{o}_{AgCuPyr\ Skn}$ in Eqn 11.

1995). As a consequence, it takes in only a limited amount of As, up to ~34% in the 300–350°C range, though this amount rapidly decreases at temperatures below 280°C. In the Appendix the α-miargyrite Ag-Cu mixing model is expanded to include As-Sb mixing parameters. Unfortunately, due to a lack of Ag-Cu exchange data along the Sb-As join between α-miargyrite and pyrargyrite both in this study and in Ghosal and Sack (1995), we are unable to evaluate the As-Sb reciprocal and reciprocal ordering parameters. Such an evaluation awaits some future study involving Ag-Cu exchange between As-bearing α-miargyrite and pyrargyrite near the Sb end of the As-Sb join between α-miargyrite and smithite.

Lastly, while the fast ion conductor properties of Ag and Cu in these sulphosalt minerals is extremely valuable in facilitating relatively rapid Ag-Cu exchange between them at temperatures going as low a 150°C, the disadvantage is that the Ag-Cu content of α-miargyrite and chalcostibite will also tend to rapidly re-equilibrate with the surrounding Ag and Cu bearing sulphosalts and sulphides as these deposits cool, ultimately to the ambient temperature of the mine itself, and thus not preserve the temperature at which the ore formed. As a consequence, their use as a geothermometer is somewhat limited.

Acknowledgements

Valuable guidance from R.O. Sack and M.S. Ghiorso is gratefully acknowledged as well as NSF grant EAR92-19085 (to R.O. Sack).

Technical assistance was provided by D. Ebel, and S. Sinha. C. Hager provided valuable support with regard to use of the microprobe. Many useful discussions were held with S. Fritz and he provided the use of a high-precision balance on which all weighing was performed.

Appendix

The mixing model for α-miargyrite may be expanded to include a limited solid solution with As as determined by Ghosal and Sack (1995). In such an expanded model, the coefficients of the second degree Taylor expansion take the form:

$$\bar{G}^* = g_o + g_{X_{Cu}} X_{Cu}^{Mrg} + g_{X_{As}} X_{As}^{Mrg} + g_s s + g_{X_{Cu}X_{Cu}} X_{Cu}^{Mrg^2} + g_{X_{As}X_{As}} X_{As}^{Mrg^2} + g_{ss} s^2 + g_{X_{Cu}X_{As}} X_{Cu}^{Mrg} X_{As}^{Mrg} + g_{X_{Cu}s} X_{Cu}^{Mrg} s + g_{X_{As}s} X_{As}^{Mrg} s \quad (A1)$$

where, in addition to those parameters already defined,

$$X_{As}^{Mrg} = \frac{As}{As+Sb} \quad (A2)$$

This results in the following expression for $\bar{G}^*$:

$$\bar{G}^* = \bar{G}^{o\ Mrg}_{AgSbS_2}(1 - X_{Cu}^{Mrg} - X_{As}^{Mrg}) + \bar{G}^{o\ Mrg}_{CuSbS_2} X_{Cu}^{Mrg} + \bar{G}^{o\ Mrg}_{CuAsS_2} X_{As}^{Mrg} + (\Delta\bar{G}_{X_{Cu}s} + W^{A\ Mrg}_{AgCu} + W^{B\ Mrg}_{AgCu}) X_{Cu}^{Mrg}(1 - X_{Cu}^{Mrg}) + W^{Mrg}_{AsSb} X_{As}^{Mrg}(1 - X_{As}^{Mrg}) + \Delta\bar{G}^*_{rec} X_{Cu}^{Mrg} X_{As}^{Mrg} + \tfrac{1}{2}(\Delta\bar{G}^*_s - (W^{B\ Mrg}_{AgCu} - W^{A\ Mrg}_{AgCu}))s + \tfrac{1}{4}(\Delta\bar{G}^*_{X_{Cu}s} - (W^{A\ Mrg}_{AgCu} + W^{B\ Mrg}_{AgCu}))s^2 + \tfrac{1}{2}\Delta\bar{G}^*_{X_{As}s} X_{As}^{Mrg} s + (W^{B\ Mrg}_{AgCu} - W^{A\ Mrg}_{AgCu}) X_{Cu}^{Mrg} s \quad (A3)$$

Here the parameters involving only Ag and Cu as well as the evaluation of the ordering parameter, s, are defined as before. Parameters involving the As-Sb join include W^{Mrg}_{AsSb} defined by Ghosal and Sack (1995) with a value of 7.0 ± 0.5 kJ/gfw, $\Delta\bar{G}_{rec}$, the reciprocal energy defined by the following relation:

$$CuSbS_2 + AgAsS_2 = AgSbS_2 + CuAsS_2 \quad (A4)$$

and $\Delta\bar{G}_{X_{As}s}$, the reciprocal ordering parameter defined by the expression:

$$Ag^A_{0.5}Cu^B_{0.5}AsS_2 + Cu^A_{0.5}Ag^B_{0.5}SbS_2 = Cu^A_{0.5}Ag^B_{0.5}AsS_2 + Ag^A_{0.5}Cu^B_{0.5}SbS_2 \quad (A5)$$

(cf. Harlov and Sack, 1994).

The molar configurational entropy, $\bar{S}^{IC}$, is also expanded to include two new terms involving the Sb-As join or:

$$\bar{S}^{IC} = -R[\tfrac{1}{2}X^A_{Cu}\ln(X^A_{Cu}) + \tfrac{1}{2}(X^A_{Ag}\ln(X^A_{Ag}) + \tfrac{1}{2}X^B_{Cu}\ln(X^B_{Cu}) + \tfrac{1}{2}X^B_{Ag}\ln(X^B_{Ag}) + X^{Mrg}_{As}\ln(X^{Mrg}_{As}) + (1 - X^{Mrg}_{As})\ln(1 - X^{Mrg}_{As})] \quad (A6)$$

This results in the following expanded expressions for the chemical potentials for α-miargyrite and its hypothetical Cu end-member ($CuSbS_2$):

$$\mu^{Mrg}_{AgSbS_2} = \bar{G}^{o\ Mrg}_{AgSbS_2} + (\Delta\bar{G}^*_{X_{Cu}s} + W^{A\ Mrg}_{AgCu} + W^{B\ Mrg}_{AgCu}) X_{Cu}^{Mrg^2} + W^{Mrg}_{AsSb} X_{As}^{Mrg^2} - \Delta\bar{G}^*_{rec} X_{Cu}^{Mrg} X_{As}^{Mrg} - \tfrac{1}{4}(\Delta\bar{G}^*_{X_{Cu}s} - (W^{A\ Mrg}_{AgCu} + W^{B\ Mrg}_{AgCu}))s^2 - \tfrac{1}{2}\Delta\bar{G}^*_{X_{As}s} X_{As}^{Mrg} s - (W^{B\ Mrg}_{AgCu} - W^{A\ Mrg}_{AgCu}) X_{Cu}^{Mrg} s + RT[\tfrac{1}{2}\ln(1 - X_{Cu}^{Mrg} - \tfrac{1}{2}s) + \tfrac{1}{2}\ln(1 - X_{Cu}^{Mrg} + \tfrac{1}{2}s) + \ln(1 - X_{As}^{Mrg})] \quad (A7)$$

and

$$\mu^{Mrg}_{CuSbS_2} = \bar{G}^{o\ Mrg}_{CuSbS_2} + (\Delta\bar{G}^*_{X_{Cu}s} + W^{A\ Mrg}_{AgCu} + W^{B\ Mrg}_{AgCu})(1 - X_{Cu}^{Mrg})^2 + W^{Mrg}_{AsSb} X_{As}^{Mrg^2} + \Delta\bar{G}^*_{rec} X_{As}^{Mrg}(1 - X_{Cu}^{Mrg}) - \tfrac{1}{4}(\Delta\bar{G}^*_{X_{Cu}s} - (W^{A\ Mrg}_{AgCu} + W^{B\ Mrg}_{AgCu}))s^2 - \tfrac{1}{2}\Delta\bar{G}^*_{X_{As}s} X_{As}^{Mrg} s + (W^{B\ Mrg}_{AgCu} - W^{A\ Mrg}_{AgCu})(1 - X_{Cu}^{Mrg}) s + RT[\tfrac{1}{2}\ln(X_{Cu}^{Mrg} + \tfrac{1}{2}s) + \tfrac{1}{2}\ln(X_{Cu}^{Mrg} - \tfrac{1}{2}s) + \ln(1 - X_{As}^{Mrg})] \quad (A8)$$

Obviously, in evaluating Cu and Ag mixing parameters for end-member α-miargyrite, the As-Sb terms drop out. The reciprocal and reciprocal ordering parameters, $\Delta\bar{G}_{rec}$ and $\Delta\bar{G}_{X_{As}s}$, are problematic. We have no real data involving Ag-Cu exchange equilibria along the limited Sb-As join between α-miargyrite and smithite (cf. Ghosal and Sack, 1995) to properly evaluate either parameter. As a consequence, while we have a value for W^{Mrg}_{AsSb} (7.0 ± 0.5 kJ/gfw; Ghosal and Sack, 1995), our inability to evaluate $\Delta\bar{G}_{rec}$ and $\Delta\bar{G}_{X_{As}s}$, does not allow for a definitive solution. By analogy with polybasite-pearceite (cf. Harlov and Sack, 1994), these terms are probably not equal to 0.

References

Birch, W.D. (1981) Silver sulphosalts from the Meerschaum mine, Mt. Wills, Victoria, Australia. *Mineral. Mag.*, **44**, 73–8.

Birch, W.D. (1992) Mineralogy of the Mt. Wills goldfield, Victoria, with emphasis on the sulphosalt minerals. *Austral. Mineral.*, **6**, 3–17.

Ghiorso, M.S. (1990) The application of the Darken equation to mineral solid solutions with variable degrees of order-disorder. *Amer. Mineral.*, **75**, 539–43.

Ghosal, S. and Sack, R.O. (1995) As-Sb energetics in argentian sulphosalts. *Geochim. Cosmochim. Acta*, **59**, 3573–9.

Grigas, I., Mozgova, N.N., Orlyukas, A. and Samulenis, V. (1976) The phase transition in $CuSbS_2$ crystals. *Sov. Phys. Crystall.*, **20**, 741–2.

Harker, D. (1936) The application of the three-dimensional Patterson method and the crystal structures of proustite, Ag_3AsS_3, and pyrargyrite, Ag_3SbS_3. *J. Chem. Phys.*, **4**, 381–90.

Harlov, D.E. (1995) *Thermochemistry of minerals in the system Ag_2S-Cu_2S-Sb_2S_3-As_2S_3*. Ph.D. dissertation, Purdue Univ., USA.

Harlov, D.E. (1999) Thermochemistry of Ag-Cu exchange equilibria between proustite, sinnerite, and pearceite: constraints on Ag-Cu and As-Sb mixing in pyrargyrite-proustite. *Eur. J. Min.* (in press).

Harlov, D.E. and Sack, R.O. (1994) Thermochemistry of polybasite-pearceite solutions. *Geochim. Cosmochim. Acta*, **58**, 4363–75.

Harlov, D.E. and Sack, R.O. (1995*a*) Ag-Cu exchange equilibria between pyrargyrite, high-skinnerite, and polybasite solutions. *Geochim. Cosmochim. Acta*, **59**, 867–74.

Harlov, D.E. and Sack, R.O. (1995*b*) Thermochemistry of Ag_2S-Cu_2S sulfide solutions: constraints derived from coexisting Sb_2S_3- and As_2S_3-bearing sulphosalts. *Geochim. Cosmochim. Acta*, **59**, 4351–65.

Hocart, M.R. (1937) Schema structural de la proustite et de la pyrargyrite. *Comptes Rendus Hebdomadaires des Seances de l'Academie des Sciences Paris*, **205**, 68–70.

Hofmann, W. (1935) Beitrag zur Kristallchemie der Sulfosalze des Arsens, Antimons und Wismuts. *Zeit. Kristallogr.*, **92**, 174–85.

Karup-Møller, S. (1974) Mineralogy of two copper-antimony-sulphide-oxide occurrences from the Ilimaussaq alkaline intrusion in South Greenland. *Neues Jahrb. Mineral. Abh.*, **122**, 291–313.

Karup-Møller, S. and Makovicky, E. (1974) Skinnerite, Cu_3SbS_3, a new sulphosalt from the Ilimaussaq alkaline intrusion, South Greenland. *Amer. Mineral.*, **59**, 889–95.

Kaspar, P., Mrazek, Z. and Ridkosil, T. (1983) Andorite, fizelyite and miargyrite; a decomposition of a natural solid solution?. *Neues Jahrb. Mineral. Abh.*, **147**, 47–57.

Kaspar, P., Ridkosil, T. and Srein, V. (1985) Silver-rich minerals from Trebsko near Pribram, central Bohemia, Czechoslovakia. *Neues Jahrb. Mineral. Mh.*, 19–28.

Kaspar, P., Ridkosil, T. and Slavicek, P. (1991) Silver minerals of the Trebesko deposit, Pribram orefield, Czechoslovakia. *Mineral. Rec.*, **22**, 209–12.

Keighin, C.W. and Honea, R.M. (1969) The system Ag-Sb-S from 600°C to 200°C. *Mineral. Deposita*, **4**, 153–71.

Knowles, C.R. (1964) A redetermination of the structure of miargyrite, $AgSbS_2$. *Acta Crystallogr.*, **17**, 846–51.

Makovicky, E. and Skinner, B.J. (1972) Crystallography of Cu_3SbS_3 (abstr.) *Winter Meet. Amer. Crystallogr. Assoc. Albuquerque, New Mexico, April, 1972*, Abstract K5.

Nakayama, E. (1986) Paragenetic and compositional variations of Au-Ag minerals in the ginguro ores from the Nebazawa mine, Gunma Prefecture. *Mining Geol.*, **36**, 511–22.

Sack, R.O. (1992) Thermochemistry of tetrahedrite-tennanite fahlores. In *The Stability of Minerals* (N.L. Ross and G.D. Price, eds.), 243–66. Chapman & Hall, London.

Sack, R.O. and Ghiorso, M.S. (1989) Importance of mixing properties in establishing an internally consistent thermodynamic database: thermochemistry of minerals in the system Mg_2SiO_4-Fe_2SiO_4-SiO_2. *Contrib. Mineral. Petrol.*, **102**, 41–68.

Smith, G.F.H. and Prior, G.T. (1907) Red silver minerals from the Binnenthal, Switzerland. *Mineral. Mag.*, **14**, 283–307.

Smith, J.V., Pluth, J.J. and Han, S. (1997) Crystal structure refinement of miargyrite, $AgSbS_2$. *Mineral. Mag.*, **61**, 671–5.

Solly, R.H. (1905) Some new silver minerals from the Binnenthal, Switzerland. *Mineral. Mag.*, **14**, 72–82.

Sugaki, A., Isobe, K. and Kitakaze, A. (1982) Silver minerals from the Sanru mine, Hokkaido, Japan. *J. Jap. Assoc. Mineral. Petrol. Econ. Geol.*, **77**, 65–77.

Sugaki, A., Kitakaze, A. and Isobe, K. (1984) On the gold-silver deposits of the Koryu mine, Hokkaido, Japan. *J. Jap. Assoc. Mineral. Petrol. Econ. Geol.*, **79**, 405–23.

Sugaki, A., Kim, O.J. and Kim, W.J. (1986) Gold and silver ores from the Geumwang mine in South Korea and their mineralization. *Mining Geol.*, **36**, 555–72.

[*Manuscript received 22 April 1998: revised 20 July 1998*]